Physico-Chemical and Mechanical Behavior of Natural Clay as a Porous Medium during Convective Drying

.

ABSTRACT

The present work consists on an experimental characterization of non-purified clay material. The survey is focused on the chemical, physical, and mechanical properties variation during the convective drying of the material. Clay identification by atomic absorption spectrophotometer and X-ray diffractometer are used to determine the exact composition. The study covers also essential physical properties of the material such as density, volume shrinkage, and porosity in one hand, and the mechanical properties: Young modulus and the parameters of viscoelastic behavior for the other hand. The novelty is the variation of the properties function of the material moisture content. The clay was identified kaolinite as major fraction. The true density is evaluated to (2685 +/- 35 kg/m^3). And Young modulus is about (15 MPa) for dried material. The results are judged to be acceptable comparing to the literature data.

Keywords: Non-purified clay; atomic absorption spectrophotometer; X-ray diffractometer; Convective drying; Density; Volume shrinkage; Porosity; Young modulus; Viscoelasticity.

1. INTRODUCTION

Clay is a raw material used in construction materials like cement, bricks, and ceramics. In Tunisia, this industry is one of the most important sectors in the national economy and it consumes huge amounts of energy. In 2011, it is estimated to 827.5 kTEP (57.4% of the national energy consumption in the industry sector). And especially, the drying process consumes 96.7 kTEP (6.7% of the national energy consumption in the industry sector) [1].

Clay is also considered as the typical inorganic raw material used for ceramic products, which are commonly manufactured using traditional methods. The demand for ceramics is increasing in several diverse fields. The application ranges from materials for house ware and buildings to highly functional materials called "fine ceramics". Drying is one of the important steps of ceramics manufacturing [2, 3]. And the modeling of drying is important to foresee the quality of the final product.

Clay brick masonry is one of the oldest and most durable construction techniques used by mankind. The manufacture of fired clay bricks can be divided generally into four stages. Firstly, the extraction of the raw material and its storage. After storage, clay is crushed and mixed with water. The resulting mix is characterized by enough plasticity to facilitate the molding. The crude clay is then dried by different processes. Generally, the drying process takes a lot of time and can still for one week or more. Finally, the hardening of the bricks in order to acquire additional resistance. The material is fired in a kiln with high temperature (more than 1000℃).

Drying is an important process step in the bricks manufacturing [3]. The drying related problems are cracks and deformations that may take place due to the volume shrinkage. Drying is usually carried out slowly, although fast drying cycles are widely industrially practiced.

The originality of this work is that it deals with non purified clay. In literature, most of works are done on purified clays such as kaolinite [4, 5] and bentonite [6]. The aim of this work is to characterize our product to collect data for the sector of bricks and ceramics manufacturing.

2. MATERIAL AND METHODS

2.1 Clay identification

Natural clay extracted from "*Tabarka*" region in Tunisia was used as a model material in this study. Firstly, the nature of this clay is identified by atomic absorption spectrophotometer (type Perkin Elmer 560) [2, 7]. Major elements are to be dosed (Si, Al, Fe, Mg, Mn, Ca, Na, and K). Secondly, the losses in ignition (Bound humidity and organic material in clay) were determined in a furnace at 1000℃. Finally, the X-r ay diffractometer is used to determine the main clay composition (quartz, kaolinite, illite, smectite, bentonite, ...) [2, 7].

2.2 Clay drying

The drying experiments were carried out in a convective drying tunnel (see Fig. 1) with wet air whose parameters (temperature, velocity, and humidity) are controlled and regulated. The clay samples are molded in a plate form with dimensions of (15*12*1.5 cm). The mass evolution during drying is taken with an electronic precision balance, then stored using an acquisition program.

The accuracy of the measurement is as follows: (0.001 g) for the mass, (0.1℃) for temperature, (0.1 m/s) for the air velocity, and (1%) for the relative humidity.

Fig. 1 Experimental setup for the convective dryer

The experimental conditions for the clay drying are presented in the table 1. Temperature variation between (40 and 60℃), and relative humid ity range (30-60%). The air velocity is fixed at (2 m/s). Initial moisture content of the clay samples is about (0.2 +/- 0.003 kg/kg dry mass).

Table 1. Experimental conditions for the convective clay drying.

Experiments	*Temperature (℃)*	*Air velocity (m/s)*	*Relative humidity (%)*	*Initial moisture content (dry basis)*
1	50	2	30	0.203
2	50	2	40	0.200
3	50	2	60	0.204
4	40	2	40	0.198
5	60	2	40	0.202

The drying curves can be modeled using some mathematical equations presented in table 2, to be fitted and to find the best model describing the drying kinetics.

Table 2. Mathematical Models of the drying curves [8]

Model Name	*Equation of the model*
Wang and Singh	$MR = 1+a.t + b.t^2$
Multiple Multiplicative Factor Model	$MR = (a.b + c.t^d)/(b + t^d)$
Henderson and Pabis	$MR = a.exp(-kt)$
Logarithmic	$MR = a.exp(-kt) + b$
Midilli equation	$MR = a.exp(-k(t^n)) + b.t$

Regression analyses of these equations were done by using regression models. The performance of the different models was evaluated using various statistical parameters such as the regression coefficient (r) and the standard error (S). These parameters can be calculated as following:

$$S = \sqrt{\frac{\sum_{i=1}^{n_{point s}} (y_i - f(x_i))^2}{n_{point s} - n_{param}}} \quad (1)$$

$$r = \sqrt{\frac{S_t - S_r}{S_t}} \quad (2)$$

$$S_t = \sqrt{\sum_{i=1}^{n_{point s}} (\bar{y} - y_i)^2} \quad (3)$$

$$S_r = \sum_{i=1}^{n_{point s}} (y_i - y(x_i))^2 \quad (4)$$

$$\bar{y} = \frac{1}{n_{point s}} \sum_{i=1}^{n_{point s}} y_i \quad (5)$$

2.3 Physical Properties

Cubic humid clay samples were molded from clay powder mixed with distilled water at a moisture content of (20%). These homogeneous samples of (1 cm^3) approximate dimension were used to determine the evolution of the density with the moisture content. They are placed in the convective dryer to reduce their humidity. Every five minutes, one sample is taken from the dryer to measure its apparent density. The experiment consists on the measurement of the sample weight in air and the corresponding buoyancy force in methanol. On the figure 2, is given a photo of the experimental apparatus mounted on a precision balance.

The corresponding moisture content of the sample is determined by the measure of the humid mass and the dry mass. All samples are placed in an oven at (105℃) during (24 hours) to eliminate all the humidity.
The true density of the solid (intrinsic density) is determined by pychnometry. A standard (50 mL) pychnometer was used in this stage. The measurements were performed in triplicate and we take the mean value.

Fig.2. Experimental apparatus for the apparent density determination installed with a precision balance.

2.3.1 Apparent density

As it is mentioned above, the apparent density is determined by measurement of the sample weight in air and the corresponding buoyancy force in methanol. The following equation (correspond to the apparatus) is used to calculate the density of all samples.
Apparent density (ρ) was determined with the principle of Archimedes. This property is calculated by using the following correlation related to the used experimental apparatus:

$$\rho = \frac{M_a\left(\rho_f - 0{,}0012\right)}{0{,}99983 * G} + 0{,}0012 \qquad (6)$$

With ρ is the apparent density, ρ_f is the fluid (methanol) density, Ma is the solid mass in air, and G is the hydrostatic buoyancy.

2.3.2 Volume shrinkage

The volume shrinkage is determined indirectly by the density measurement. There is a relation between specific volume and density:

$$R_v = \frac{V(X)}{V_0} = \frac{\rho^0\left(1+X\right)}{\rho\left(1+X^0\right)} \qquad (7)$$

2.3.3 Porosity

To calculate the gas porosity of the presented formulation uses, through Eq. 8, the following properties of the medium: initial moisture content, initial density and true density [9].

$$\Phi_g = \frac{Z-\left(1-\Phi_0\right)Y}{Z} \qquad (8)$$

Note that Z is the experimental shrinkage, Y is the ideal shrinkage (Eq. 9), Φ_0 is the initial porosity of the medium (Eq. 10) and β is the ratio of the solid true density and the liquid one (Eq. 11).

$$Y = \frac{\rho_0}{1+X_0}\left(\frac{1}{\rho_s^s} + \frac{1}{\rho_l^l}\right) \quad (9)$$

$$\Phi_0 = 1 - \frac{\rho_0}{\rho_s^s}\left(\frac{1+\beta X_0}{1+X_0}\right) \quad (10)$$

$$\beta = \frac{\rho_s^s}{\rho_l^l} \quad (11)$$

2.4 Mechanical Properties

This experimental work is introduced in order to approach the phenomena of elasticity and viscoelasticity attributed to the clay material. Many experiments were carried out to identify the parameters related to the viscoelasticity and deepen the knowledge of the structure of clays (Natural clay extracted from "*Tabarka*" region in Tunisia was used as a model material in this study). The physico-chemical analysis of the samples was carried out using X-ray diffractometry. It shows that the major fraction of clay is kaolinite.

2.4.1 Compression test: Methodology

The compression test is done to evaluate the Young Modulus of the material. Fine-grained unpurified clay powder was saturated with distilled water to produce slurry. This mixture of (30%) water content was subsequently thoroughly stirred to ensure complete homogenization of the slurry. The material is molded in cylindrical shape (27 mm diameter and 10 mm height).

Samples were tested using a traction-compression machine (LRX Plus) with console (Ref. No. 01/2962) shown in Figure 3. It served to determine the modulus of elasticity (Young's modulus) of the clay with a test speed equal to (0.1 mm/min).

Fig.3. Traction compression machine (LRX Plus) with console (Ref. No. 01/2962).

2.4.2 Parameters of the viscoelastic behavior

The viscoelastic nature of the clay can be studied by examining the temporal evolution of the clay's response following a set of tests such as the relaxation, the creep or oscillating stresses. Since the clay is considered as a solid and remains until the end of the drying, the Kelvin Voigt model is the best choice to describe its behavior [10-11].

The viscoelastic behavior can be presented using rheological models using springs (elastic character) and dashpots (viscous character) linked in series or in parallels.

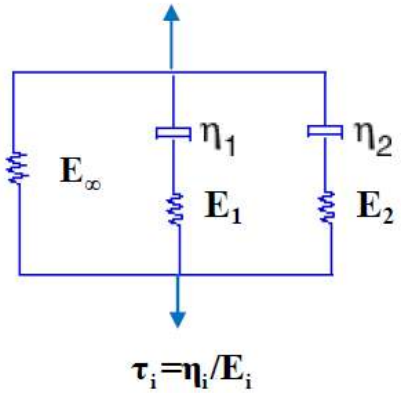

Fig.4. Rheological model for clay [13].

The experimental study conducted for the rheological characterization of the clay is derived from an application of a constant strain using the same traction-compression machine. Depending on water content, the results show that the relaxation level of equilibrium is reached for times greater than 10 hours. Relaxation time is higher for the more sample is dried. The viscosity significantly decreases within water content. In fact, the liquid phase escape is used to relax the solid matrix. According to works in the rheology field which have shown that the delay time (after creep) is higher than relaxation time [12], the values of the relaxation time experimentally quantified were considered for the move to increase with delay time (result of creep test).

3. RESULTS AND DISCUSSION

3.1 Clay identification

If we examine table 3, we can conclude that the major fraction of the clay is silica. It is also rich in Iron, Aluminium, and Potassium. The other compounds are negligible of about 2.5 %. The losses in ignition are also important due the nature of clay (natural: non purified).
The results of the X-ray diffractometer are presented in figure 5. From the figure above, it is clear that the major fraction of the crystalline phase is quartz and kaolinite.

Table 3. Chemical composition of clay in mass percentage.

Oxides	*SiO_2*	*K_2O*	*Al_2O_3*	*Fe_2O_3*	*Na_2O*	*CaO*	*MgO*	*MnO*	*L. I.*
Mass %	39.400	15.612	13.848	14.102	0.679	1.142	0.566	0.128	14.440

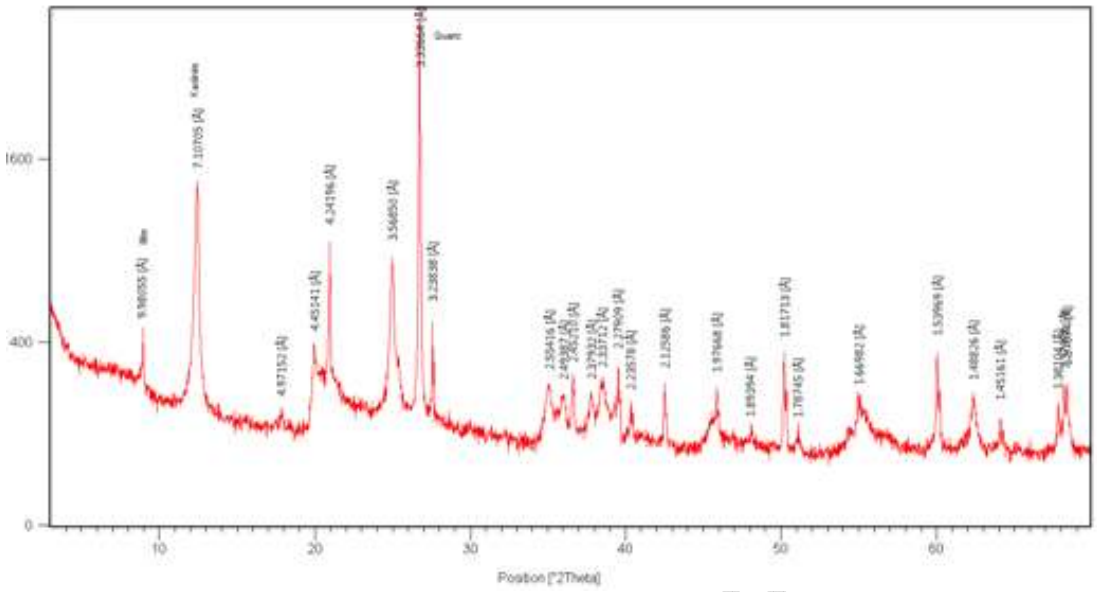

Fig. 5. X-ray diffraction pattern for clay

3.2. Drying Kinetics

The results of the convective drying kinetics of clay at the different experimental conditions are presented in Figure 6. The drying time is about 22 hours.

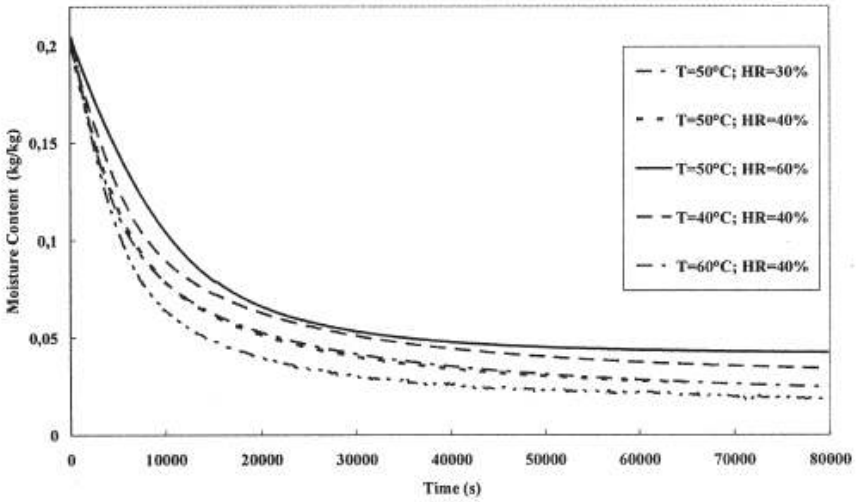

Fig. 6. Drying of clay at different conditions

3.3. Density, Volume shrinkage, and Porosity

The results of the density variation with the moisture content are presented on the figure 7. For the true density of the clay is evaluated to (2685 +/- 35 kg/m^3).

The volume shrinkage is plotted in Fig.8. It reflects a good prediction of this parameter. The difference is within the pattern established for the (2D) simulation model contrary to the nature of this parameter (3D).

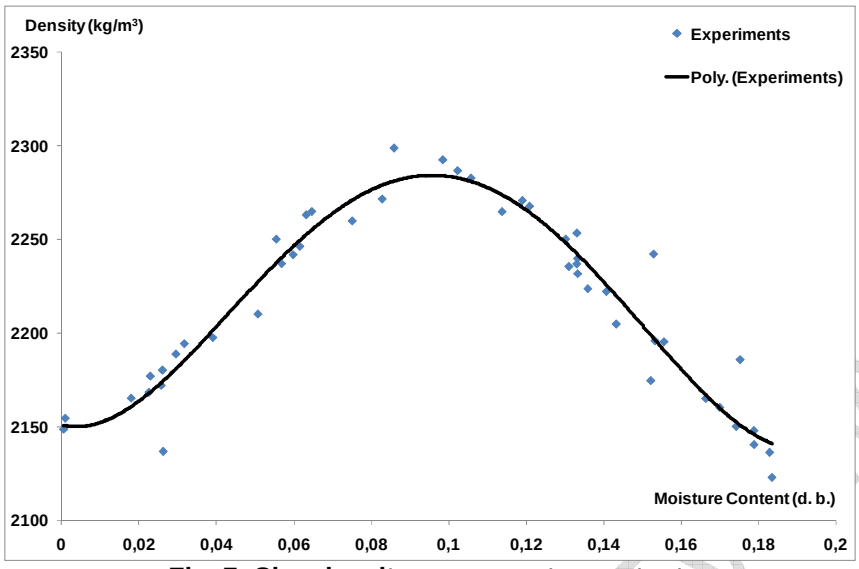

Fig. 7. Clay density versus water content.

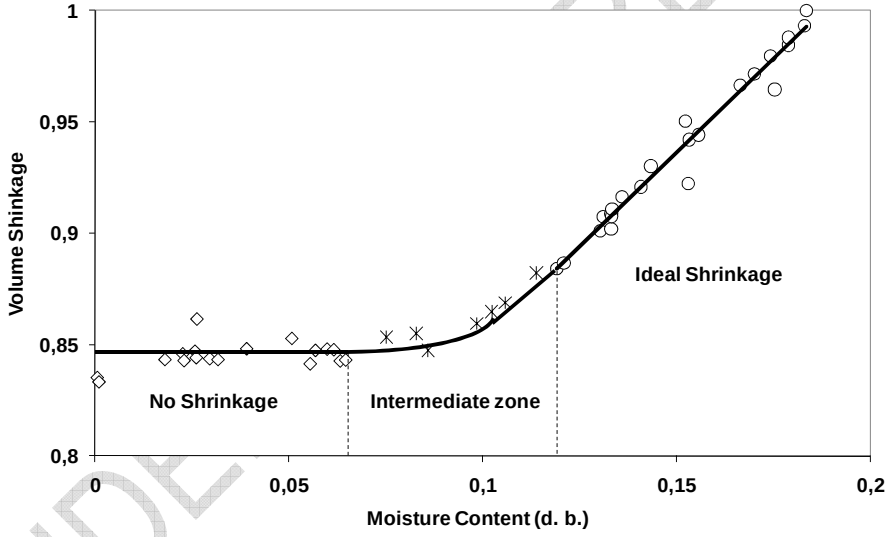

Fig. 8. Volume shrinkage versus moisture content

As it is still a validation of a model proposed by referring to the experimental study, the constants used for this study are:

$\rho_0 = 2123\ kg/m^3$; $\rho_s^s = 2685\ kg/m^3$; $\rho_l^l = 1000 \frac{kg}{m^3}$; $X_0 = 0.1835\ kg/kg$.

From Fig.8, the water content decreases highlighting a gap in the structure of the material filled with a volume shrinkage increasing to register a water content using the presence of a third phase other than the solid and liquid. The gas begins to be in the material pores. Figure 9 shows that this phase is negligible up to water content nearly equal to 0.086 (saturated medium). Then, the medium becomes unsaturated and the air porosity increases quickly to 20% for dry material.

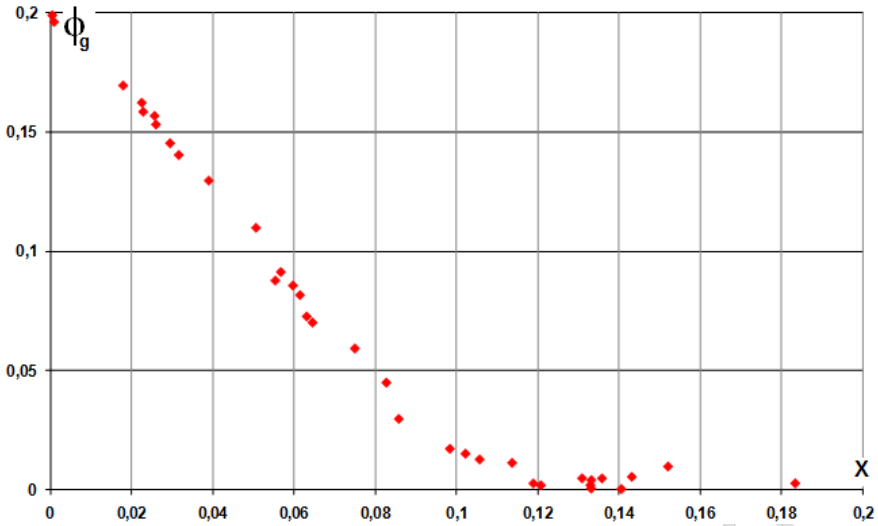

Fig.9. Porosity gaseous ratio versus water content.

3.4. Young modulus and viscoelastic parameters

The response of the material to compression is a function of the water content. This result matches with those obtained in the literature [14]. For a range of water contents close to 15%, the clay behaves pure elastic. For water contents close to 30%, the material behaves like a non-linear elastic medium. For water contents below 10%, the clay is similar to the behaviour of brittle materials: the stress tends to increase much in the deformation range of elastic domain. Note that the drop in stresses corresponds to visible cracks on the sample tested faces.

Unlike what is common to the relations linearity to determine the Young modulus, the evolution of stresses-strains depends on what is small or large deformations hypothesis. To distinguish different modulus of elasticity, we adopt the following citation [15]: “In the first zone, designated as elastic, the modulus reaches a value almost independent of the level of distortion. Deformations are very small in this area. Therefore the modulus is generally described as ‘maximum’ or ‘initial’ (Emax). In the following areas, the modulus decreases with increasing deformations. Monotonic curves are described by a ‘secant’ modulus (Esec) defined by the slope of the line connecting the origin to the current module. And a tangent one (Etan) determined by the slope of the curve in neighborhood of the point”.

Al Husein [16] introduced, as well, the difficulty of choosing the deformations modules. In referring to his thesis (soils and geotechnical): “it’s often advisable to take a medium modulus, for example the one corresponding to a level equal to 50% of diverter at break”.

The question that arose at this stage of the study was the level of strains to be considered always to ensure a result on the elastic domain. In the case of Mrani work [17], the agar gel’s elasticity modulus is calculated from the average slope of the lines for loading and unloading. Characterization of this modulus, in the work of Pourcel [18] on the alumina gel, was based on calculating the slope between 1 and 3% strains. Kowalski et al., [14] worked on the kaolin’s elastic modulus by determining this characteristic in a strain equal to 0.2%. The choice of Collard [19] regarding the line slope of 0 to 1% strain was chosen in our work. Note that Collard used plates of clay of the same composition as ours, as reference material. We chose to present the secant Young Modulus versus moisture content in figure 10. The curve presented is the result of the fitting model.

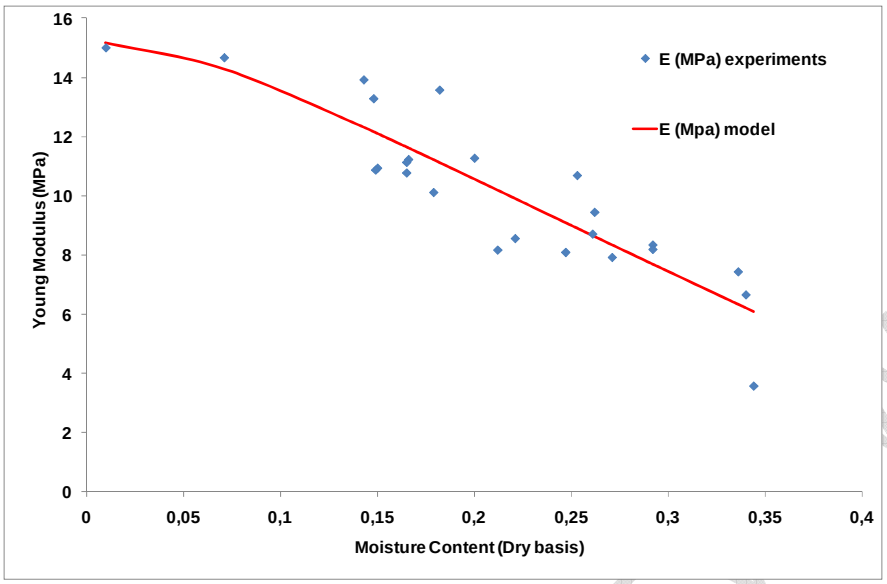

Fig. 10. Evolution of the secant Young modulus of the clay versus water content.

This evolution can be presented by the following relation between Young modulus and moisture content:

$$E(X) = a - b\,e^{(-c\,X^{-d})} \quad (12)$$

With: a=15.187; b=423.83; c=2.79; and d=0.3.

Experimental relaxation tests are presented in figure 11.

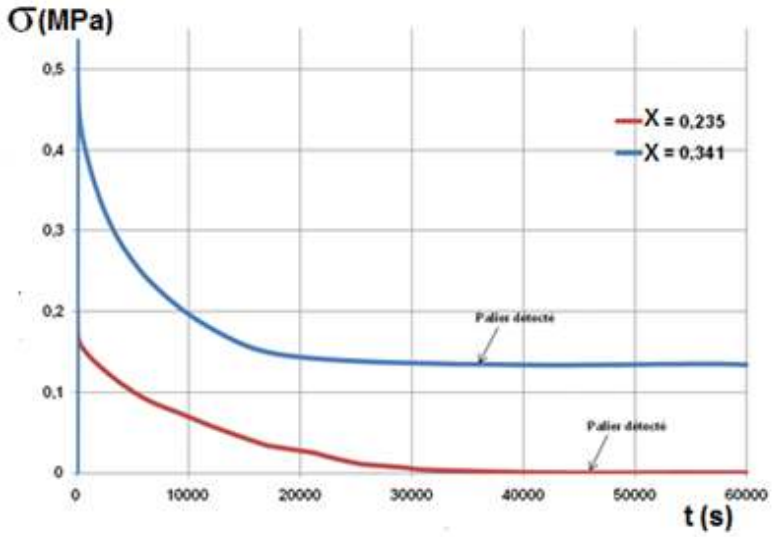

Fig. 11. Relaxation function curves at different moisture content.

The results of fitting the experimental data for relaxation function using a Prony series gives:

$$E(t) = E_0 + E_1 e^{1/\tau_1} + E_2 e^{1/\tau_2} \quad (13)$$

With: E0=0.018 MPa; E1=0.21 MPa; E2=0.66 MPa; τ1= 40 s; and τ2= 4500 s.

4. CONCLUSION

This paper presents some essential properties of natural clay material to understand its behavior during the convective drying process. Clay identification by atomic absorption spectrophotometer and X-ray diffractometer was shown kaolinite as the major fraction. The main results of this study are: clay density, volume shrinkage and porosity are determined versus its moisture content. The true density is evaluated to (2685 +/- 35 kg/m^3). Young modulus decreases with moisture content and it is about (15 MPa) for the dried material. The viscoelastic behavior of the material is underlined via the relaxation function determined experimentally.

REFERENCES

1. Agence Nationale des Energies Renouvelables, *Energy Audit Report*, Tunisia, 2011.

2. Chemkhi, S., Zagrouba, F., Bellagi, A. Drying of ceramics: modelling of the thermo-hydro elastic behavior and experiments, *Industrial Ceramics.* 2005: 25 (3): 149-156.

3. Gong, Z.X., Mujumdar, A.S., Itaya, Y., Mori, S., Hasatani, M. Drying of clay and nonclay media: heat and mass transfer and quality aspects, *Drying Technology*, 1998: 16 (6), pp 1119-1156.

4. Chemkhi, S., Zagrouba, F., Bellagi, A. Thermodynamics of water sorption in clay, *Desalination*, 2004: 166, 393-399.

5. Chemkhi, S., Zagrouba, F. Development of Darcy-flow model applied to simulate the drying of shrinking media, *Brazilian Journal of Chemical Engineering*, 2008: 25 (3): 503-514.

6. Mihoubi, D., Bellagi, A. Thermodynamic analysis of sorption isotherms of bentonite, *Journal of Chemical Thermodynamics*, 2006: 38: 1105-1110.

7. Usman, M.A., Ekwueme, V. I., Alaje, T. O., Mohammed, A. O. Characterization, Acid Activation, and Bleaching Performance of Ibeshe Clay, Lagos, Nigeria. *ISRN Ceramics*. Volume 2012, Article ID 658508, 5 pages.

8. Kemp, I.C., Fyhr, B. C., Laurent, S., Roques, M.A., Groenewold, C.E., Tsotsas, E., Sereno, A.A., Bonazzi, C.B., Bimbenet, J.J., Kind, M. Methods for processing experimental drying kinetics data, *Drying Technology*, 2001: 19 (1): 15-34.

9. Madiouli, J., Lecomte, D., Nganya, T., Chavez, S., Sghaier, J., and Sammouda, H. A Method for Determination of Porosity Change from Shrinkage Curves of Deformable Materials, *Drying Technology*. 2007: 25 (4): 621-628.

10. Hasatani M., Itaya Y., Hayakawa K. Fundamental study on shrinkage of formed clay during drying: viscoelastic strain-stress and heat moisture transfer. *Drying Technology*, 1992: 10, (4), pp 1013-1036.

11. Bulicek, M., Malek, J., Rajagopal, K.R. On Kelvin-Voigt model and its generalizations, Research team 1. Center for Mathematical Modeling, Mathematical Institute of the Charles University, Sokolovska, 2010: 1-8.

12. Witasse, R., Georgin, J.F., Reynouard, J.M., Berthollet, A., Dauffer, D., Chauvel, D. Contribution for modelling creep and drying shrinkage of reinforced concrete structures. *Structures and Materials*. 2000: 6, 577-586.

13. Hammouda, I., Mihoubi, D., Modelling of drying induced stress of clay: elastic and viscoelastic behaviours. *Mechanical Time-dependent Materials*. 2014: 18(1), 97-111.

14. Kowalski, S.J., Banaszak, J., Rybicki, A. Plasticity in materials exposed to drying. *Chemical Engineering Science*, 2010: 65: 5105-5116.

15. Nguyen Pham, P.T. Etude en place et au laboratoire du comportement en petites déformations des sols argileux naturels. Ph.D. Thesis, École Nationale des Ponts et Chaussées, France, 2008.

16. Al Husein, M. Étude du comportement différé des sols et ouvrages géotechniques. Ph.D. Thesis, University Alep, Syria, 2001.

17. Mrani, I., Bénet, J.C., Fras, G., Zrikem, Z. Two dimensional simulation of dehydration of a highly deformable gel: Moisture content, stress and strain fields. *Drying Technology*, 1997: 15 (9): 2165-2193.

18. Pourcel, F., Jomaa, W., Puiggali, J. R., Rouleau, L. Crack Appearance during Drying of an Alumina Gel: Thermo-Hydro-Mechanical Properties. *Drying Technology*, 2007: 25 (5): 759-766.

19. Collard, J.M., Arnaud, G., Fohr, J.P. The drying-induced deformations of a clay plate. *International Journal of Heat and Mass Transfer*, 1992: 35 (5), pp 1103-1114.